

Electrochemical performance of r-graphene oxide based MnO₂ nanocomposite for supercapacitor

S. Kalaiarasi^{1,2}, S. Shyamala³, M. Kavitha³, C. Vedhi³, R. R. Muthuchudarkodi³

¹Manonmaniam Sundaranar University, Tirunelveli, Tamilnadu, India

²PG and Research Department of Chemistry, A.P.C. Mahalaxmi College for Women, Thoothukudi, Tamilnadu, India

³PG and Research Department of Chemistry, V.O. Chidambaram College, Thoothukudi, Tamilnadu, India

Corresponding author: R. R. Muthuchudarkodi, muthu.rajaram@gmail.com, cvedhi23@gmail.com

ABSTRACT In this study, we improved the capacitance of carbon based reduced graphene oxide (rGO) and metal oxide based MnO₂ by preparing nanocomposites of rGO/MnO₂ nanocomposite using chemical synthesis method. The prepared nanoparticles and nanocomposites are characterized by FTIR spectroscopy, XRD, PL spectroscopy and FESEM with EDAX spectroscopy. FTIR studies disclose the characteristic chemical bonding between the respective materials. The FESEM images demonstrate that the surface structure of rGO and MnO₂ can be easily tuned by forming the composite of rGO/MnO₂ materials leading to excellent process ability of the system. The super capacitive behaviors of nanocomposites are evaluated using cyclic voltammetry and galvanostatic charge–discharge techniques. The specific capacitance of rGO/MnO₂ composite is high compared to that of MnO₂ nanoparticle. In addition, impedance measurements of the MnO₂ nanoparticles and rGO/MnO₂ electrodes are executed proposing that the rGO/MnO₂ composite electrodes are promising materials for super capacitor (186.6 Fg⁻¹).

KEYWORDS graphene oxide, cyclic voltammetry, nanocomposite, FESEM, electrochemical properties, supercapacitors

ACKNOWLEDGEMENTS The authors would like to express their gratitude to the Department of Science and Technology (FAST TRACK and FIST) in New Delhi, India for allowing them to use the CHI electrochemical workstation. The FT-IR spectra were generously provided by the PG and Research Department of Chemistry at V. O. Chidambaram College in Thoothukudi. We are grateful to the Secretary of A. P. C. Mahalaxmi College for Women, Thoothukudi.

FOR CITATION Kalaiarasi S., Shyamala S., Kavitha M., Vedhi C., Muthuchudarkodi R. R. Electrochemical performance of r-graphene oxide based MnO₂ nanocomposite for supercapacitor. *Nanosystems: Phys. Chem. Math.*, 2022, **13** (3), 320–330.

1. Introduction

Recently, great interest appeared in fabricating and utilizing novel graphene oxide–metal oxide nanocomposites for environmental remediation by the degradation and elimination of toxic organic contaminants and heavy metals, and for antibacterial applications. Compared with graphene oxide, graphene oxide–metal oxide nanocomposites show a unique structural morphology and photochemical properties which render them good candidates for water treatment projects [1]. Many research groups are working on the nanocomposite materials particularly graphene-based composite materials. Different types of graphene based composite materials are being investigated and reported for various engineering applications [2].

Supercapacitors have attracted growing interest, due to their high power density, long cycle life, and fast charging rate, which play an important role in complimenting or even replacing batteries in many applications [3–5]. Nevertheless, the low-energy density and higher production cost are still some of the major challenges for implementing supercapacitor in future application. To date, the carbon materials (activated carbon, carbon nanotubes, (CNT) and reduced graphene oxide (rGO)) [3,4,6] transition metal oxides (ruthenium dioxide (RuO₂), manganese dioxide (MnO₂), nickel oxide (NiO), cobalt oxide (Co₃O₄) [4,5,7] and conducting polymers (polypyrrole, polyaniline, PEDOT-PSS and polythiophene) [8,9] have been recognized as the most promising materials for supercapacitors. Based on literature, the carbon-based electrodes display an excellent rate of capability, good reversibility [3], and superior cyclability but suffer from low capacitance value. On the other hand, transition metal oxides and polymer-based electrodes produce high capacitance through a fast faradic reaction but have a poor rate of capability and stability [3,10].

Transition metal oxides are used in supercapacitor applications. In transition metal oxide, RuO₂ exhibits major supercapacitive performance, but it cannot be commercialized due to its high production cost and toxicity. Low cost

and high theoretical specific capacitance materials, like manganese oxide, ferrous oxide and nickel oxide have been used as electrode materials for supercapacitor [11–13]. However, the electrical conductivity of these metal oxides limits on its power density and cycling stability. Out of these metal oxides, manganese oxide is a most stable oxide and it has a number of significant applications as electrochemical material, high density magnetic storage medium, active catalyst, ion-exchange, Li–Mn–O rechargeable batteries, etc. [14]. Reduced graphene oxide has high specific surface area, which is highly desirable in catalysis, and acts as a two dimensional support for metallic nanoparticles with high dispersion [15]. In addition, it has a high adsorption capacity, defects in its structure that can generate new surface functionalities and increase the interactions with the metal nanoparticles [16, 17] and excellent mechanical properties that allow one to reach high stability and durability, increasing the lifetime of the catalyst. In this work, we report on the synthesis of nanostructured composites, consisting of manganese oxide anchored on rGO, by the one-step chemical synthesis method. The prepared samples were investigated by UV-Vis, FTIR, XRD, Field Emission Scanning Electron Microscope (FESEM) with EDAX spectroscopy and Photoluminescence spectroscopy. The electrochemical properties of these materials are evaluated by cyclic voltammetry, charge-discharge method and impedance techniques.

2. Material and methods

2.1. Material

All reagents used were of analytical grade, obtained from Merck (India) Ltd and used as received without further purification. Graphite, potassium permanganate, phosphoric acid, H₂O₂, manganese sulphate, concentrated hydrochloric acid, potassium hydroxide, sodium hydroxide and deionized water were used to synthesis of MnO₂ nanoparticles and rGO/MnO₂ nanocomposites.

2.2. Synthesis of MnO₂ nanoparticles

For the co-precipitation method, the manganese salt, manganese (II) sulphate of 0.2 M, dissolved in double distilled water with continuous stirring at a constant temperature of 80 °C. 2 M of NaOH solution was added while stirring until the pH of the solution reached 12. The stirring was continued at a constant temperature of 80 °C for 1 hour. The resulting brown precipitate was then filtered and washed with ethanol.

2.3. Synthesis of rGO/MnO₂ nanocomposite

In the present work, reduced graphene oxide (rGO) was produced using modified Hummer's method from pure graphite powder. 0.2 g of rGO was dispersed in 100 mL water by ultra-sonication up to 30 min to separate out a single sheet of graphene oxide. To synthesize in situ rGO/ MnO₂ nanocomposites, subsequently, 0.2 M (100 mL) of manganese (II) sulphate was added and sonicated for another 30 min, followed by drop wise addition of 1M potassium hydroxide solution under stirring for 1 h. This mixture was stirred well and refluxed for 2 h, which resulted in the formation of black colour reduced graphene oxide decorated MnO₂ nanocomposite. The precipitate was separated from the reaction mixture, washed several times with deionised water and followed by washing with ethanol to remove the impurities. Finally, the obtained product was dried at room temperature [18]. Fig. 1 shows that Synthesis of rGO/MnO₂ nanocomposite.

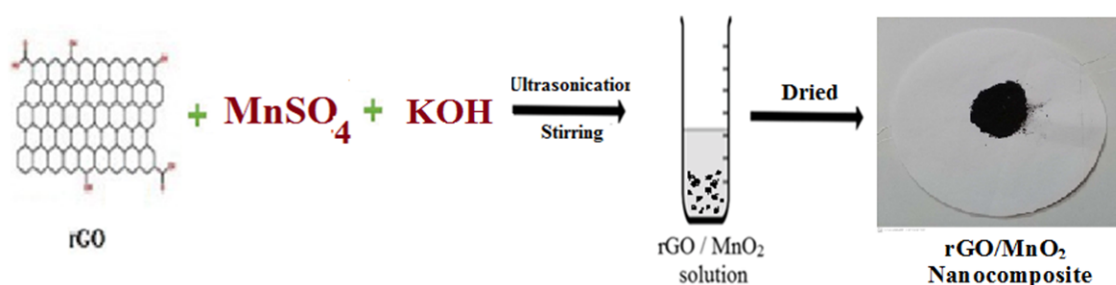


FIG. 1. Preparation method of rGO/MnO₂ nanocomposite

2.4. Characterization

Computer controlled Thermo Scientific Instrument with iD Transmission (Model P4600) was used to record the FTIR spectra, which was then followed by the KBr pellet method. Photoluminescence (PL) Spectra of the samples were recorded on a spectrofluorometer (JASCO, FP8300). The computer controlled XRD system JEOL IDX 8030 was used to record the X-ray diffraction of samples. EDAX and FESEM measurements were carried by JEOL JSM-6700F field emission scanning electron microscope. The electrochemical behaviors of nanocomposites have been investigated through CH-Instrument Inc., TX, and USA.

3. Result and discussion

3.1. FTIR analysis

The FTIR spectra disclose the chemical information and major functional groups existing in the MnO₂ nanoparticles and rGO/MnO₂ materials. Fig. 2 shows FTIR spectra of MnO₂ nanoparticles and rGO/MnO₂ nanocomposites. The broad band observed at 3421 cm⁻¹ is assigned to the symmetric stretching vibrational mode of hydroxyl groups in the MnO₂ nanoparticles and rGO/MnO₂ nanocomposites [19]. The bands at 1460.56, 1461.39, 1635.79, and 1680.42 cm⁻¹ indicate the presence of C–OH groups and water molecules in the both prepared samples. The two narrow and strong absorption bands at 642 and 540 cm⁻¹ are assigned to the pairing mode between Mn–O stretching modes. The FTIR spectrum for rGO/MnO₂ nanocomposites is depicted in Fig. 2(b) which denotes the peaks corresponding to the wave numbers 2324, and 516 cm⁻¹ denoting the presence of functional groups such as C–H, C–OH, O–Mn–O, respectively. These characteristic bands confirm the formation of rGO, MnO₂ nanoparticles and rGO/MnO₂ nanocomposites [20].

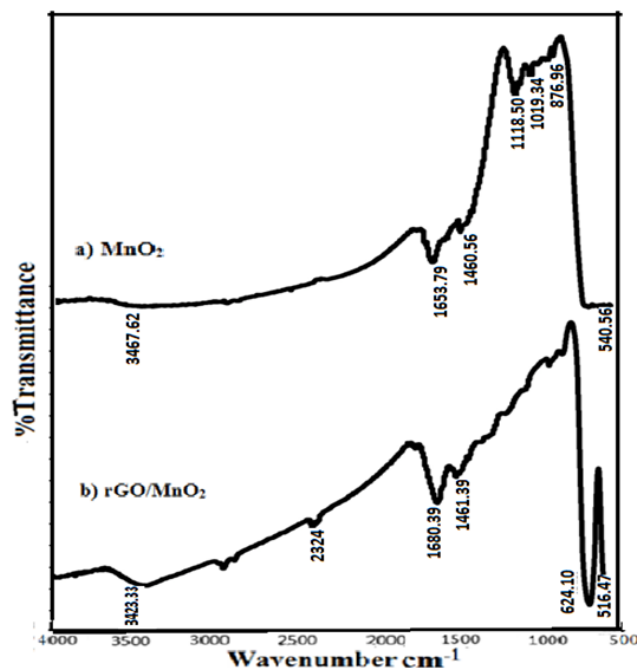


FIG. 2. FT-IR spectra of a) MnO₂ nanoparticles, b) rGO/MnO₂ nanocomposite

3.2. X-Ray diffraction analysis

The crystal structures of MnO₂ nanoparticles and rGO/MnO₂ nanocomposite are characterized by XRD. As can be seen in Fig. 3(a), all the diffraction peaks of pure MnO₂ nanoparticles indicate the tetragonal structure JCPDS (044-0141). The good crystallization is proved by its reflection peak. The XRD pattern for MnO₂ nanoparticles is depicted in the diffraction peaks at (110), (101), (211), (221) and (311) corresponding to 2θ values 29.4, 37.4, 46.0, 55.6 and 63.30. Fig. 3(b) shows the XRD patterns of rGO/MnO₂ nanocomposites. The XRD patterns of rGO/MnO₂ nanocomposite showed diffraction peaks at 29.0, 32.5, 36.1, 44.4, 58.4 and 69.90, and a phase with a rhombohedral structure was formed (JCPDS 96-500-0208) [21]. The main crystallite sizes of the rGO based metal oxide nanocomposite are calculated using the Debye–Scherrer formula (eq. (1)):

$$D = \frac{k\lambda}{\beta \cos \theta}, \quad (1)$$

where λ is the wavelength of radiation used (1.54060 Å for CuK α radiation), k is the Scherrer constant equal to 0.94, β is the full width at half maximum (FWHM) intensity of the diffraction peak for which the particle size is to be calculated, θ is the diffraction angle of the diffraction peak in question and D is the crystalline size in nanometers (nm). The average crystallite sizes of MnO₂ nanoparticles and rGO/MnO₂ nanocomposite are determined to be 47.1 and 40 nm, respectively.

3.3. FESEM and energy dispersive X-Ray analysis (EDAX)

The surface morphological studies of nanoparticles and nanocomposites were performed by FESEM analysis. The elements of deposits on MnO₂ nanoparticles and rGO/MnO₂ nanocomposite are also studied using EDAX spectrum. Figs. 4(a,b,c) and 4(a,b,c) show the FESEM image, EDAX spectrum and Elemental distribution of MnO₂ nanoparticles and rGO/MnO₂ nanocomposites. The FESEM images of MnO₂ nanoparticles are portrayed in Fig. 4(a). It is well

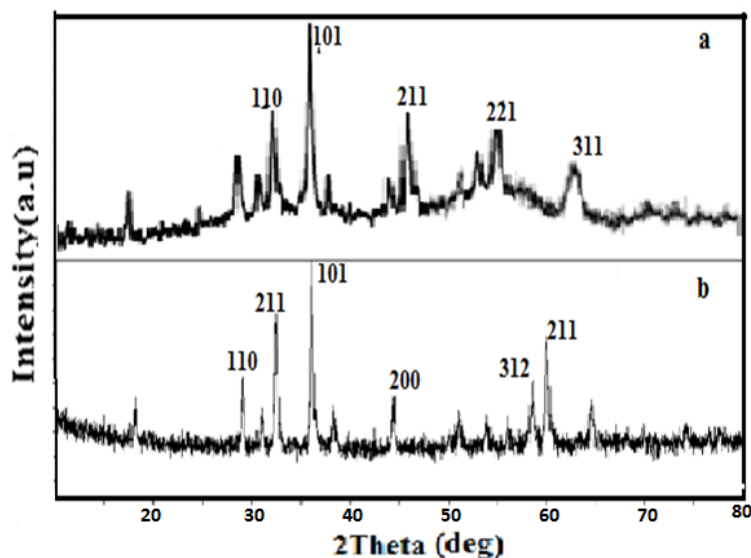


FIG. 3. XRD pattern of a) MnO₂ nanoparticles, b) rGO/MnO₂ nanocomposites

documented that the surface morphology has significant impact on the performance of nanostructure materials. The uniform distributions of grains are observed in the micrographs. The particles are nearly spherical in shape and has uniform size (one micron) [18]. The presence of atomic composition manganese (34 %) and oxygen (66 %) are confirmed as observed from the EDAX (Fig. 4(c)) spectrum. The chemical composition and product purity of the MnO₂ nanoparticle was examined by EDAX. The elemental mapping of MnO₂ nanoparticles are shown in Fig. 4(c). The highest amount of manganese (Mn) is distributed in the whole surface compared to that oxygen.

Figure 5(a) shows the surface morphologies of synthesized rGO/MnO₂ nanocomposites. It looks like the combination of flakes (sheet like structure) and spheres indicating the collaboration of rGO and MnO₂ nanocomposites [20]. The EDAX pattern of rGO/MnO₂ nanocomposites materials from Fig. 5(b) confirms that the synthesized materials show predominant peaks of C, O and Mn elemental peaks only. The respective EDAX spectra confirm the presence of carbon element along with the rGO/MnO₂ nanocomposites [22]. The elemental mapping of rGO/MnO₂ nanocomposites is shown in Fig. 5(c). There are large amount of oxygen (O) which is distributed on the surface in Fig. 5(c) compared to that carbon and manganese surface [23].

3.4. Photoluminescence study

The optical properties of MnO₂ nanoparticles, and rGO/MnO₂ nanocomposites were studied by using the photoluminescence spectra analysis. To investigate the efficient separation of charge carriers in the nanocomposites, photoluminescence (PL) spectroscopy was carried out to reveal the migration, transfer, and recombination processes of photo induced electron/hole pairs. The excitation source employed here was the 370 nm. Fig. 6(a) shows that pure MnO₂ nanoparticles have emission peak at 412 nm. However, the emission peak of the rGO/MnO₂ nanocomposite is much lower than that of the pure MnO₂ nanoparticles indicating that the addition of graphene leads to the PL quenching. The lowest recombination of the electron-hole pair is achieved by rGO/MnO₂ nanocomposites where it shows the lowest emission intensity among all. As shown in Fig. 6, the PL intensity decreases successively in the order of MnO₂ nanoparticles, and rGO/MnO₂ nanocomposites. The emissions was mostly attributed to the radiative transition between the electron and the hole recombination process [24].

3.5. Electrochemical studies

Electrochemical measurements of cyclic voltammetric studies were conducted using a CHI 650c electrochemical workstation with conventional three electrode cell at room temperature. Modified MnO₂ and rGO/MnO₂-glassy carbon electrode for comparison, was employed as the working electrode. Silver/silver chloride (Ag/AgCl) electrode acted as the reference electrode and platinum wire as the counter electrode. The electrochemical properties of the MnO₂ nanoparticles, and rGO/MnO₂ nanocomposites were investigated by means of cyclic voltammetry (CV) with potential window from 0.3 to 0.7 V at pH 7 (phosphate buffer solution). The CV curve of synthesized nanomaterials with different scan rate such as 100, 50, 30, 20, 10 and 5 mV/s are shown in Fig. 7(a–c). Strong redox behavior of metal oxides and asymmetric variation is observed during the lower scanning rate. However, beyond scan rate, nearly rectangular smooth CV loops are observed with mild redox behavior due to the presence of rGO. It is found that the current increases when the scan rate is increased, which indicates the good capacitance behavior of the nanocomposite.

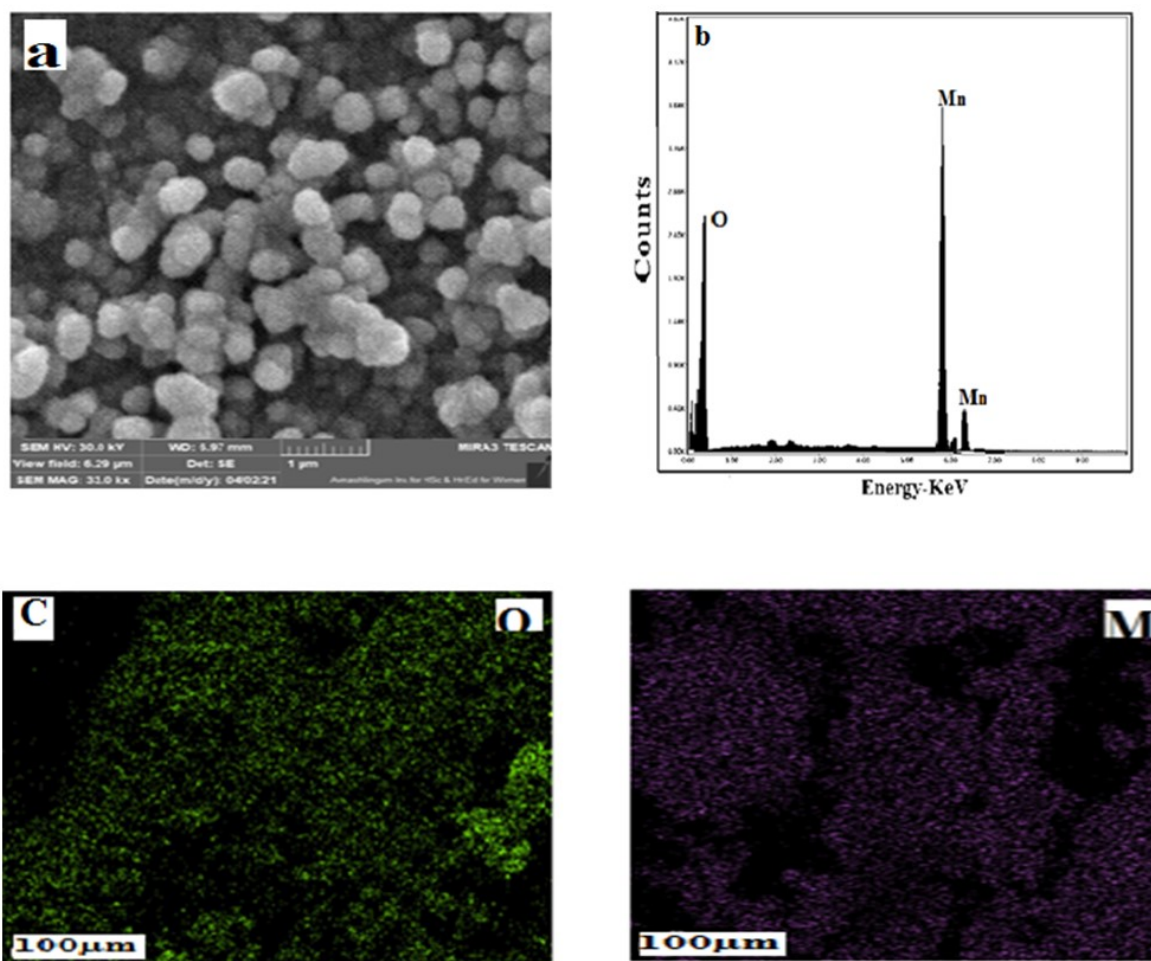


FIG. 4. a) FESEM image; b) EDAX spectrum; c) element mapping of Mn and O of the MnO₂ nanoparticles

3.6. EIS investigation of electrochemical behavior of nanoparticle and nanocomposite

The Nyquist plots of the modified nanoparticles and nanocomposites were studied using EIS. Randles' equivalent circuit model was used to fit experimental parameters such as the electron transfer resistance (R_{ct}), the solution resistance (R_s) and the double layer capacity (C_{dl}). Fig. 8 shows the real and imaginary parts of the electrochemical impedance spectra for the bare glassy carbon electrodes (GCE), MnO₂ nanoparticles, and rGO/MnO₂ nanocomposites modified GCE recorded at pH 7. The rGO/MnO₂ nanocomposites modified GCE shows small semicircular region with very high electron transfer resistance value compared to that of bare and MnO₂ nanoparticle of GCE electrode, indicating the low conductivity of the nanocomposite. These results show that the rGO/MnO₂ nanocomposites have very good electrochemical activity compared with the bare GCE. The composite could therefore be efficiently used for various electrocatalytic reactions. Table 1 shows that impedance parameters such that R_s , R_{ct} and C_{dl} values of bare, MnO₂ nanoparticles and rGO/MnO₂ nanocomposites.

TABLE 1. Impedance parameters such that R_s , R_{ct} and C_{dl} values of bare, MnO₂ nanoparticle, and rGO/MnO₂ nanocomposite

Samples	R_s (Ω)	R_{ct} (Ω cm ²)	C_{dl} (μ F cm ⁻²)
Bare GCE(Glassy Carbon Electrode)	7.928	7140	0.0014
MnO ₂ Nanoparticles	24.16	12110	0.0036
rGO/MnO ₂ Nanocomposite	15.21	34125	0.0023

The phase angle against frequency plot termed as Bode plot articulates about the capacitive character. The maximum phase angle of rGO/MnO₂ nanocomposite (73 °) strongly demonstrates the capacitive nature [25] compared to that for MnO₂ nanoparticles (71 °) as displayed in Fig. 9. Now, electrochemical performance in scale of mechanical flexibility is

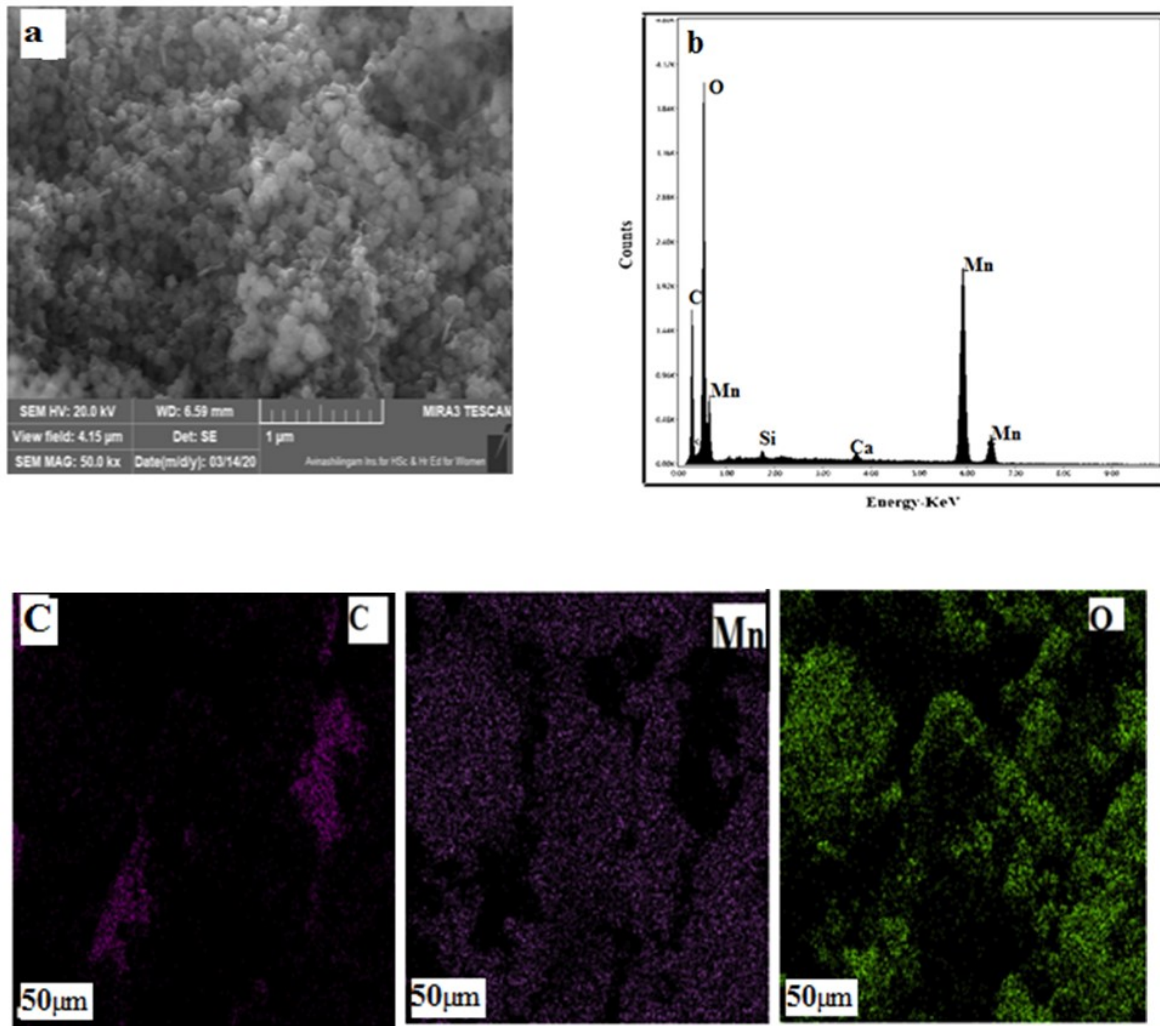


FIG. 5. a) FESEM image; b) EDAX spectrum; c) element mapping of C, Mn and O of the rGO/MnO₂ nanocomposite

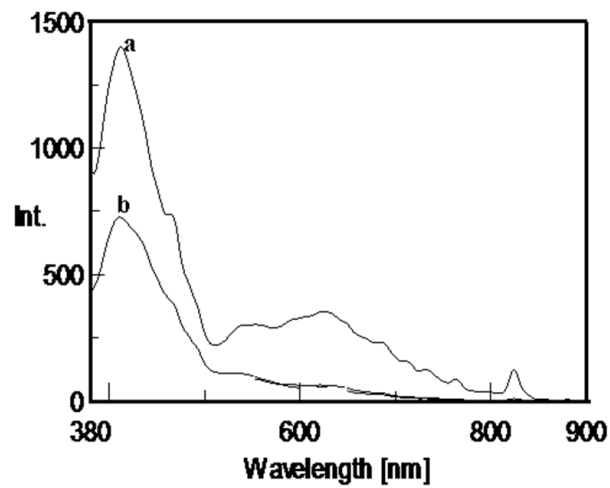


FIG. 6. PL spectrum of a) MnO₂ nanoparticles; b) rGO/MnO₂ nanocomposite

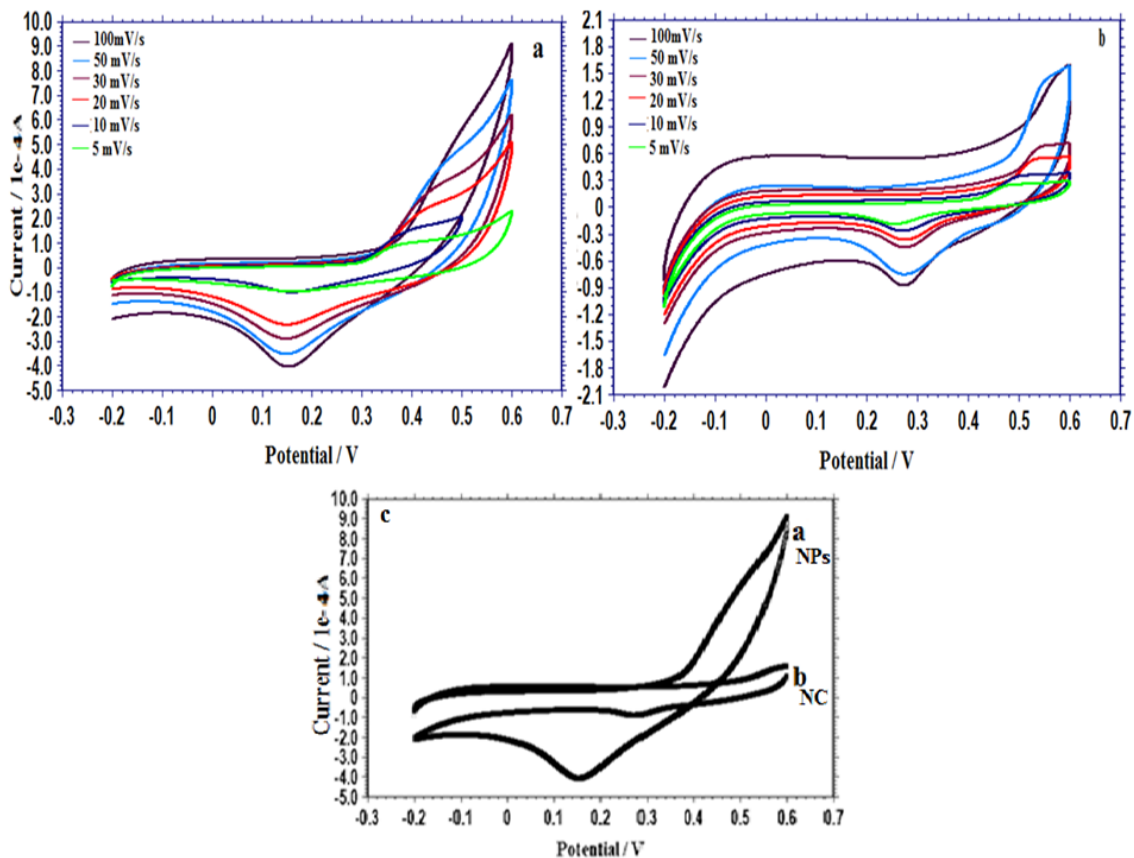


FIG. 7. Cyclic voltammetric behavior of a) MnO_2 nanoparticles; b) rGO/MnO_2 nanocomposites at different scan rate in pH 7; c) MnO_2 nanoparticles and rGO/MnO_2 nanocomposites at scan rate 100 mV/s

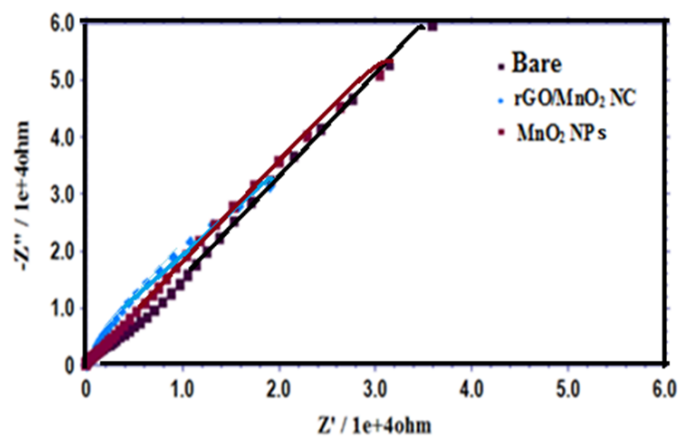


FIG. 8. Electrochemical Impedance spectra of MnO_2 nanoparticles and rGO/MnO_2 nanocomposite

an important tool to implement its application towards portable electronics. Investigation of flexibility was carried out by bending the device from 0 to 175 °.

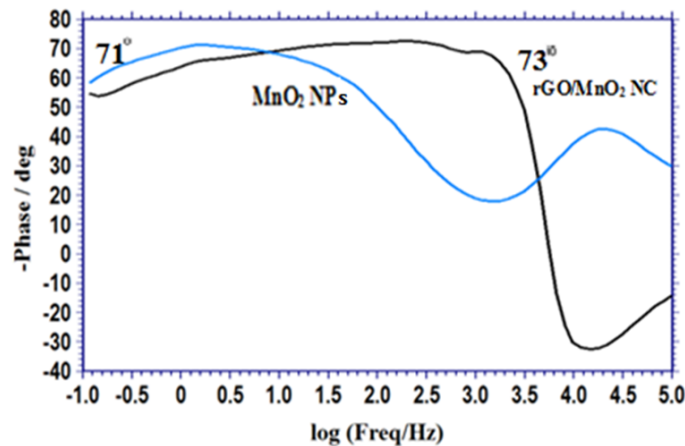


FIG. 9. Bode plot of $-$ phase angle/deg. versus $\log (f/\text{Hz})$ for MnO₂ nanoparticles and rGO/MnO₂ nanocomposite

3.7. Galvanostatic charge-discharge behaviour of the MnO₂ nanoparticle and rGO/MnO₂ nanocomposite

The galvanostatic charge-discharge method is essential for assessing supercapacitor performance and long-term stability. A formula (eq. (2)) can be used to calculate the discharge specific capacitance from the discharge curve. The galvanostatic charge-discharge behaviour of MnO₂ nanoparticles and rGO/MnO₂ nanocomposite with a variable constant current density such as 0.1, 0.3 and 0.5 Ag⁻¹ in the potential range of 0.5 to 1 is depicted in Fig. 10. Specific capacitances of the electrodes were calculated from charge-discharge curves using the following equation:

$$C_s = \frac{I\Delta t}{m\Delta V}, \quad (2)$$

where I (A) is the discharge current, Δt (s) is the discharge time, m is the mass of the electroactive material (g), and ΔV is the potential window (V). At constant current density of 0.1 Ag⁻¹, the specific capacitances obtained from charge-discharge curves of MnO₂ nanoparticles and rGO/MnO₂ nanocomposite are 92.5 and 186.5 Fg⁻¹, respectively. As a result, the rGO/MnO₂ nanocomposite has good capacitive behaviour during the charge-discharge process. The comparison results clearly show that our newly prepared nanocomposite electrode outperforms several others. One of the important factors influencing the capacitive behavior of the supercapacitor is the current density. The prepared samples' charge-discharge curves were performed at pH 7. With increasing current densities, the specific capacitance gradually decreases. This takes place due to the low utilization of electroactive materials at high discharge current densities, as ions in the electrolyte are unable to enter the active material's inner surface, leaving only the active material's outer surface.

In addition, the power density and energy density are important parameters for the investigation of the electrochemical performance of the electrochemical cells. They have been used to evaluate the performance of the hybrid rGO/MnO₂ composite electrode. The power density and energy density can be calculated from the following equations (eqs. (3) and (4)).

$$E = \frac{1}{2}C\Delta V^2, \quad (3)$$

$$P = \frac{E}{t}, \quad (4)$$

where, P (Wkg⁻¹), C (Fg⁻¹), Δ (V), t (s) and E (Whkg⁻¹) are the power density, specific capacitance, potential window of discharge, discharge time and energy density, respectively. Tables 2 and 3 show the calculated specific capacitance, energy and power density values. The plots of specific capacitance, current density, power density, and energy density can be seen in Fig. 11(a,b). Fig. 11(b) depicts the maximum power density of the rGO/MnO₂ nanocomposite versus nanoparticles. These findings support the use of MnO₂ nanoparticles and rGO/MnO₂ nanocomposite as potential materials for energy storage applications. The electrochemical stability of supercapacitors is critical for their use in practical applications.

4. Conclusion

In this study, chemical synthesis was used to successfully prepare MnO₂ nanoparticles and an rGO/MnO₂ nanocomposite. The phase purity of the synthesized nanoparticles and nanocomposites is confirmed by the X-ray diffraction pattern. FTIR is used to confirm the presence of surface functional groups on MnO₂ nanoparticles and the rGO/MnO₂

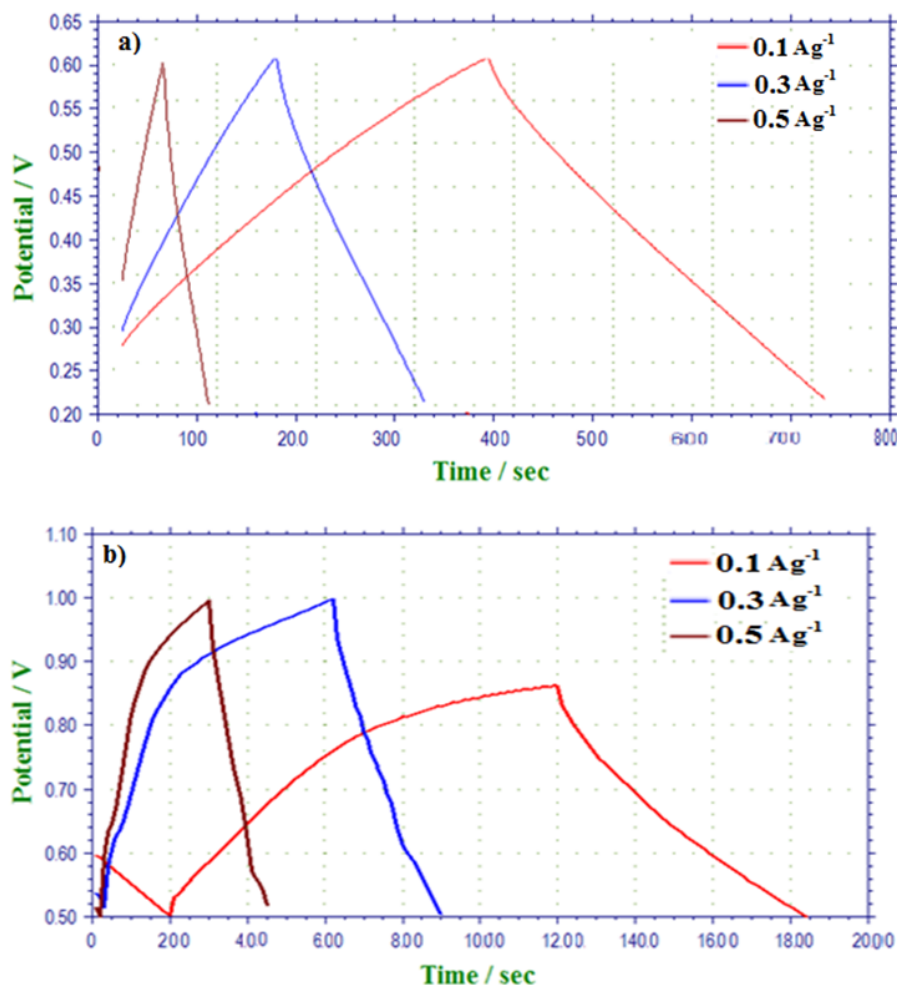


FIG. 10. Galvanostatic charge-discharge curves of a) MnO_2 nanoparticles; b) rGO/MnO_2 nanocomposite at different current densities in pH 7

TABLE 2. Various values of specific capacitance (F/g), energy (Wh/kg) and Power density (W/kg) obtained for MnO_2 nanoparticle at different current density

Current Density (Ag^{-1})	0.1	0.3	0.5
Specific capacitance (Fg^{-1})	92.5	89	85
Energy Density (Whkg^{-1})	7.4	7.12	6.8
Power Density (Wkg^{-1})	64	142.4	320

TABLE 3. Various values of specific capacitance (F/g), energy (Wh/kg) and Power density (W/kg) obtained for rGO/MnO_2 Nanocomposite at different current density

Current Density (Ag^{-1})	0.1	0.3	0.5
Specific capacitance (Fg^{-1})	186.6	180	160
Energy Density (Whkg^{-1})	22	20	17
Power Density (Wkg^{-1})	160.2	247.4	426.6

nanocomposite. The X-ray diffraction pattern confirms the phase purity of the synthesized nanoparticle and nanocomposite. FESEM analysis confirms the nanosize of MnO_2 nanoparticles and rGO/MnO_2 nanocomposite. PL spectra revealed the change of luminescence intensity in the rGO/MnO_2 nanocomposite are compared to the MnO_2 sample with almost

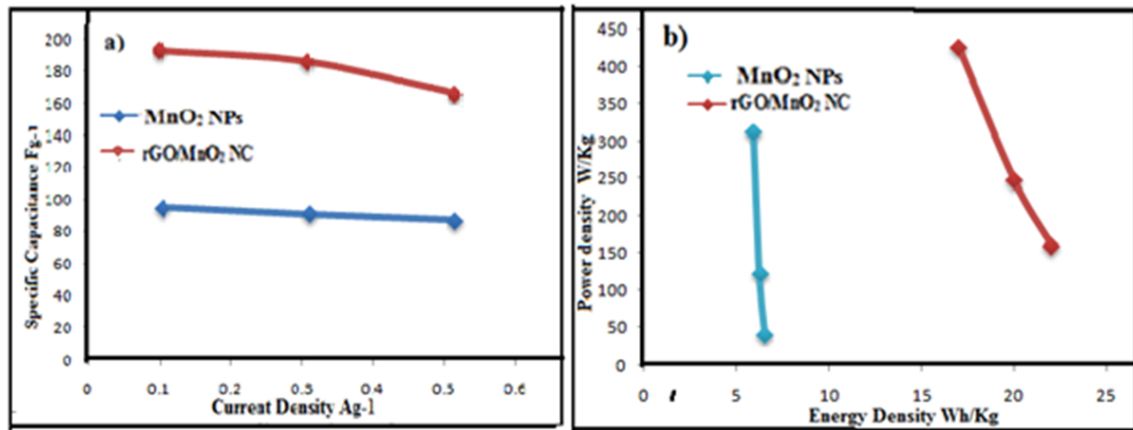


FIG. 11. a) Specific capacitances of MnO₂ nanoparticles and rGO/MnO₂ nanocomposite versus different current densities; b) Plot of power density versus energy density of MnO₂ nanoparticles and rGO/MnO₂ nanocomposite

linear decrease in excitation intensity. The specific capacitance of the rGO/MnO₂ nanocomposite was discovered to be higher than that of pure MnO₂ nanoparticles. In (phosphate buffer solution) pH 7, the two samples showed distinct capacitances at different current densities. The energy density and power density of the rGO/MnO₂ nanocomposites are higher than those of the MnO₂ nanoparticles. The nanocomposite's relatively high energy density and power density ensure that it acts as an efficient supercapacitor.

References

- [1] Li Q., Zhan Z., Jin S., Tan B. Wetttable Magnetic hyper cross linked microporous Nanoparticle as an efficient adsorbent for water treatment. *Chem. Eng. J.*, 2017, **326**, P. 109–116.
- [2] Chandra V., Park J., et al. Water dispersible magnetite reduced graphene oxide composites for arsenic removal. *ACS Nano*, 2010, **4** (7), P. 3979–3986.
- [3] Wanlu Yang, Zan Gao, et al. Synthesis of reduced graphene nanosheet/urchin-like manganese dioxide composite and high performance a super capacitor electrode. *Electrochim. Acta*, 2012, **69**, P. 112–119.
- [4] Li Wang, Yaolin Zheng, et al. Three-Dimensional Kenai Stem-Derived Porous Carbon/MnO₂ for High-Performance Supercapacitors. *Electrochim. Acta*, 2014, **135**, P. 380–387.
- [5] Wei W., Cui X., Chen W., Ivey D.G. Manganese oxide-based materials as electrochemical supercapacitor electrodes. *Chem. Soc. Rev.*, 2011, **40** (3), P. 1697–1721.
- [6] Bordjiba T., Belanger D. Development of new nanocomposite based on nanosized-manganese oxide and carbon nanotubes for high performance electrochemical capacitors. *Electrochim. Acta*, 2010, **55** (9), P. 3428–3433.
- [7] Wang H., Gao Q., Hu J. Asymmetric capacitor based on superior porous Ni–Zn–Co oxide/hydroxide and carbon electrodes. *J. Power Sources*, 2010, **195** (9), P. 2419–3046.
- [8] Snook A.G., Kao P., Best A.S. Conducting-polymer-based supercapacitor devices and electrodes. *J. Power Sources*, 2011, **196** (1), P. 1–12.
- [9] Farah Alvi, Manoj K. Ram, et al. Graphene–polyethylene dioxythiophene conducting polymer nanocomposite based supercapacitor. *Electrochim. Acta*, 2011, **56**, P. 9406–9412.
- [10] Qian Yang, Qi Li, et al. High performance graphene/manganese oxide hybrid electrode with flexible holey structure. *Electrochim. Acta*, 2014, **129**, P. 237–244.
- [11] Wei W., Cui X., Chen W., Ivey D.G. Manganese oxide-based materials as electrochemical supercapacitor electrodes. *Chemical Society Reviews*, 2011, **40**, 1697.
- [12] Hu C.C., Wu Y.T., Chang K.H. Low-Temperature Hydrothermal Synthesis of Mn₃O₄ and MnOOH Single Crystals: Determinant Influence of Oxidants. *Chemistry of Materials*, 2008, **20**, 2890.
- [13] Toupin M., Brousse T., Belanger D. Charge storage mechanism of MnO₂ electrode used in aqueous electrochemical capacitor. *Chemistry of Materials*, 2004, **16**, 3184.
- [14] Dubal D.P., Dhawale D.S., Salunkhe R.R., Pawar S.M., Lokhande C.D. A novel chemical synthesis and characterization of Mn₃O₄ thin films for supercapacitor application. *Applied Surface Science*, 2010, **256**, 4411.
- [15] Hu M., Yao Z., Wang X. Graphene-Based Nanomaterial for Catalysis. *Ind. Eng. Chem. Res.*, 2017, **56**, P. 3477–3502.
- [16] Julkapli N.M., Bagheri S. Graphene supported heterogeneous catalysts: An overview. *Int. J. Hydrogen Energy*, 2015, **40** (2), P. 948–979.
- [17] Machado B.F., Serp P. Graphene-based materials for catalysis. *Catal. Sci. Technol.*, 2012, **2** (1), P. 54–75.
- [18] Nagi M. Graphene oxide–metal oxide nanocomposites: fabrication, characterization and removal of cationic rhodamine B dye. *RSC Advances*, 2018, **8** (24), P. 13323–13332.
- [19] Farahmandjou M. Simple synthesis of new nano-sized pore structure vanadium pentoxide (V₂O₅). *Int. J. Bio-Inorg. Hybr. Nanomater.*, 2015, **4** (4), P. 243–247.
- [20] Yugambica S., Clara Dhanemozhi A., Iswariya S. Synthesis and characterization of MnO₂/rGO nanocomposite for supercapacitors. *Int. Research J. of Engineering and Technology (IRJET)*, 2017, **4** (2), P. 486–491.
- [21] Wyckoff R.W.G. The Crystal Structures of Some Carbonates of the Calcite Group. *American J. of Science*, 1920, P. 317–360.
- [22] Shihao Huang. Development of Graphene Based Nanocomposite for Supercapacitor Applications, Ph.D thesis. School of Materials Science and Engineering Faculty of Science, University of New South Wales, 2019.

- [23] Gadang Priyotomo, Siska Prifiharni, et al. A Field Study Of Atmospheric Corrosion Of Carbon Steel After Short Exposure In Palauan Ratu, West Java Province, Indonesia. *Walailak J. Sci. & Tech.*, 2021, **18** (17), 9667.
- [24] Sadiq M.J.M., Shenoy U.S., Bhat K.D. Synthesis of BaWO₄/NRGO-g-C₃N₄ nanocomposites with excellent multifunctional catalytic performance via microwave approach. *Front. Mater. Sci.*, 2018, **12**, P. 247–263.
- [25] Yadav A.A., Lokhande C.A., et al. The synthesis of multifunctional porous honey comb-like La₂O₃ thin film for supercapacitor and gas sensor applications. *J. Colloid Interface Sci.*, 2016, **484**, P.51–59.

Submitted 2 April 2022; revised 5 April 2022; accepted 28 May 2022

Information about the authors:

Senthurpandi Kalaiarasi – Research scholar (Reg. No.18222232032025), PG and Research Department of Chemistry, V. O. Chidambaram College, Thoothukudi, (Affiliated to Manonmaniam Sundaranar University, Tirunelveli, Tamilnadu, India); PG and Research Department of Chemistry, A.P.C. Mahalaxmi College for Women, Thoothukudi, Tamilnadu, India; kalaponpriya@gmail.com

Sudalaimani Shyamala – PG and Research Department of Chemistry, V.O. Chidambaram College, Thoothukudi, Tamilnadu, India; sruthsam1@gmail.com

Murugan Kavitha – PG and Research Department of Chemistry, V.O. Chidambaram College, Thoothukudi, Tamilnadu, India; Kavithamurugam25@gmail.com

Chinnapaiyan Vedhi – PG and Research Department of Chemistry, V.O. Chidambaram College, Thoothukudi, Tamilnadu, India; cvedhi23@gmail.com

Rajaram R. Muthuchudarkodi – PG and Research Department of Chemistry, V.O. Chidambaram College, Thoothukudi, Tamilnadu, India; muthu.rajaram@gmail.com, cvedhi23@gmail.com

Conflict of interest: the authors declare no conflict of interest.